CLOSE BINARY MASS ANOMALIES AND METALLICITY[1]

W. VAN HAMME
Rijksuniversiteit te Gent, Sterrenkundig Observatorium; Department of Astronomy, University of Florida, Gainesville; and
School of Sciences, University of South Carolina Coastal Carolina College

AND

R. E. WILSON
Department of Astronomy, University of Florida, Gainesville
Received 1985 May 1; accepted 1986 January 17

ABSTRACT

It has been asserted that frequently noted differences between directly observed (i.e., radial velocity) and inferred (spectral type, luminosity class) masses are due to systematic observational errors, and that the errors depend on spectrographic dispersion. Since there has been little or no progress in understanding these errors, we examine here the possibility that they may not exist, or at least that they are not the main causes of anomalous mass results. Specifically, we ask whether statistical biases and individual strong discrepancies might be explained by extreme high or low metallicity and by evolutionary age. We also ask whether certain selection effects might be important. We have recalibrated the [Fe/H] versus Strömgren m_1 relation in three ranges of spectral type, using the most current data. We have corrected the contact binary data for luminosity exchange, the rotational luminosity drop, and aspect effect. We find many mass anomalies larger than those alleged to be due to systematic velocity measurement errors, so that effect seems insufficiently large to cover all cases, even if it turns out to be real. The shift is not an effect of line blending, which *reduces* measured masses, because the results found here are in the sense of increased radial velocity masses. We give our results in terms of graphs of [Fe/H] versus mass discrepancy. The graphs appear to show the expected dependence of mass discrepancy on chemical composition, although it would be helpful to have more data on low-metallicity stars. We compute the theoretical relation in such a graph by differencing published tables of stellar models. We find a systematic shift of observed points in the sense that direct masses are larger than indirect masses, in qualitative agreement with expectations. In fact, some binaries lie well into the region which should contain only post–main-sequence stars. However, the result is found for *all* spectrographic dispersions—not only low dispersions. The shift is enhanced for the lowest dispersions but otherwise shows no clearcut dependence on dispersion. The enhancement at low dispersion might be due to systematic observational errors, but we also discuss a selection effect by which a statistical bias may result from the systematic nonpublication of low mass determinations. Another selection effect, which would be dispersion-independent, is that systems which are little evolved are relatively unlikely to show eclipses. We are doubtful that the problem lies with the stellar models, because they show good agreement with a recent empirical mass–spectral type relation. If the larger shifts are real, rather than due to systematic errors or selection effects, we may be seeing a new kind of evidence for luminosity reduction due to fast rotating cores.

Subject headings: radial velocities — stars: eclipsing binaries — stars: W Ursae Majoris

I. INTRODUCTION

It is a rather frequent experience to find that one or both components of a luminosity class V close binary have measured masses in substantial disagreement with those expected for main-sequence stars. In fact, this happens so often for some classes of binaries that it has become almost standard practice to assume that one or more kinds of ill-defined instrumental errors are to blame, and that the correct masses are those predicted by peripheral evidence—usually the two-dimensional spectral classification. Experts in radial velocity work seem to agree (many private communications) that some effect indeed exists which introduces systematic measurement errors into radial velocity curve amplitudes, especially for stars of middle to late spectral class. However the nature of this effect (photographic? psychological?) is never clearly stated. The effect is not one of line blending, which *decreases* directly

measured masses. Only a few brief discussions of the phenomenon can be found in the literature (e.g., Popper 1965, 1967), but it seems to be well known among stellar spectroscopists. In particular, it is "common knowledge" that radial velocity curve amplitudes depend on spectrographic dispersion, such that one overestimates masses from low-dispersion plates. This state of affairs is highly unsatisfactory, since we can hardly expect quantitative studies of the alleged instrumental effect to be forthcoming when even the roughest statements about its actual nature are absent from the journals. We can, however, proceed under a very different hypothesis—that the effect does not exist—and look into the possibility of explaining at least some of the examples in terms of known astrophysical effects. The most obvious such effects are those of unexpected chemical composition and of evolutionary age, both of which cause apparently anomalous effective temperatures for a given mass. Effective temperature, in turn, is commonly taken as the primary indicator of expected mass for luminosity class V stars because it is directly and fairly accurately determinable

through spectral classification and color indices. As a third alternative, one should be alert for selection effects. If it can be shown that the apparent mass anomalies are not instrumental in origin, then a large body of existing but neglected observational data will become available for effective use.

In the following sections we compare direct (radial velocity) and indirect (spectral type, luminosity class) mass determinations for luminosity class V binaries. We are interested in the following questions:

   a) Are there statistical biases or apparently irreconcilable individual discrepancies or both in the data?

   b) If so, can they be explained by astrophysical effects, such as chemical composition (population type) and age differences?

   c) After correction for chemical composition effects, and statistical allowance for age effects, are there residual discrepancies which could only be due to other astrophysical effects, to instrumental effects, or to selection effects?

To draw briefly on our results, we do find, in a few binaries, need for at least one additional astrophysical effect, which we suspect to be fast core rotation. We believe that some remaining evidence for systematic observational errors is more likely the result of selection effects rather than an instrumental effect.

II. AVAILABLE DATA BASE AND NECESSARY CORRECTIONS

We are to test the assertion that systematic errors in radial velocity masses are the cause of the mass discrepancies. We do this by accounting explicitly for chemical abundance effects and implicitly for age effects, and then checking whether any remaining differences between observed and expected masses depend statistically on spectrographic dispersion. As mentioned in § I, it is commonly believed, especially among spectroscopists, that amplitudes of radial velocity curves are systematically wrong if too low a spectrographic dispersion is used, but such an effect is rather seldom explicitly mentioned in papers and has never been quantified or explained in terms of photographic or other instrumental effects. For instance, Popper (1965) reported a systematic difference in the sum of semiamplitudes, $K_1 + K_2$, related to dispersion. Higher dispersions gave lower $K_1 + K_2$ values, and consequently lower masses, for WZ Oph and UV Leo, although not for VZ Hya. We have not found any more extensive study than this one, in which two binaries showed the effect while a third did not. In a review paper, Popper (1967) stated that systematic effects in measured velocities will be present if inadequate dispersion is used. To quote Popper: "The usual effect, well known to workers in this field, is that the separation of lines is greater on lower dispersion plates." Actually there are four separate questions involved here, which we now address.

The first question is whether a dependence of velocity amplitude on dispersion has been demonstrated in the published literature. Since the paper by Popper (1965) contains the only serious discussion of the effect which is known to us, we restrict our remarks to that work. In Popper's paper, error estimates are given for only two of six quoted $K_1 + K_2$ values, so we have only limited possibilities for checking statistical significance. Let us define quantities $K = K_1 + K_2$ and $Q = K_L/K_H$, where L and H refer to low dispersion and high dispersion respectively. One can show that errors propagate according to

$$\delta Q = \frac{1}{K_H} [(\delta K_L)^2 + Q^2 (\delta K_H)^2]^{1/2} , \qquad (1)$$

assuming that K_H and K_L are statistically independent. One can therefore find from Popper's 20 Å mm^{-1} and 40 Å mm^{-1} results for WZ Oph that $Q = 1.03 \pm 0.02$ s.d., which differs from unity by only a marginally significant amount. If we use the 75 Å mm^{-1} data from Sanford (1937), quoted by Popper, the effect is larger ($Q = 1.09$; mass error factor $= Q^3 = 1.28$), but with no error estimates we cannot know the significance of these numbers. For the other star, UV Leo, $Q = 1.11$ and $Q^3 = 1.37$, but again no standard deviations are given. Therefore, although there seems to be an indication of a real instrumental effect, one cannot now say that the existence of this "well-known" effect is established beyond question, at least in the published literature.

The second question is that of whether a significant instrumental effect exists, regardless of whether or not it has so far been demonstrated. We have in mind a future study which should determine whether such an effect is expected, but it goes far beyond the scope of the present paper.

The third question is prompted by the sizes of the above mass error (Q^3) factors, the largest of which corresponds to a 37% mass error. Popper's mass anomalies are smaller than those which often occur and cause so much consternation to binary star workers. The data tables and figures of the present paper show that 50% discrepancies are not unusual for the lowest dispersion measures, and for a few we are dealing with factors of nearly 2. In fact, for the metal-deficient binary RT Scl, Rafert and Wilson (1984) found direct masses which seem about a factor of 2 too small. Such a result is in accord with a metallicity explanation, but not with radial velocity measurement errors, which supposedly always give excess direct mass. Therefore we need to ask if, assuming that there actually are instrumental errors, as described above, are they by themselves large enough to account for the typical mass anomalies? Thus it may eventually be established that there are indeed dispersion-dependent radial velocity errors, and *also* important astrophysical effects, which together account for the mass anomalies. However, on the basis of our results it seems that astrophysical effects, if not the only agents, are at least more important than instrumental effects.

The fourth question asks whether selection effects may be important. We shall argue that they probably are, so that even without astrophysical explanations, statistical biases may not necessarily be attributable to systematic errors of measurement. This point will be discussed in greater detail in § V.

All relevant data are given in this section. Binary systems were selected either for being double-lined spectroscopic and eclipsing binaries or for being single-lined with fairly well determined (photometric) mass ratio and inclination. Only systems labeled as luminosity class V objects were included, so that each has at least one component on the main sequence. All binaries were required to have measured m_1 indices on the Strömgren system. Table 1 lists the selected detached and semidetached systems and their observed spectral types, which can be either direct estimates for the hotter components, or just estimates of combined spectral type. Figure 1 gives an overview of the velocity-mass versus spectral type–mass comparison for our selected detached and semidetached systems. In a few cases the real spectral type of the hotter star might be earlier than the estimate by a few spectral subclasses, but usually the light of the secondary is too weak to influence the combined spectral type appreciably, or the temperature of the two components are nearly equal, so that we may safely assign the classified type to the primary component. Any effects due

MASS ANOMALIES

TABLE 1

Spectral Type Data for Selected Detached and Semidetached Binaries

System	Spectral Type Primary	Combined Spectral Type	Reference	Adopted Spectral Type	M_1(Sp.)($M_\odot$)
X Tri[a]		A5V-A7V	Hill et al. (1975)	A6V	1.66
RZ Cas[a]		A2V	Olson (1968)	A2V	1.94
		A2V	Hill et al. (1975)		
		A2V	Duerbeck, Hänel (1979)		
XY Cet		A2-F0	Popper (1971b)	A8.5V	1.49
		F4V	Hill et al. (1975)		
TV Cet		F2	Popper (1968)	F2V	1.31
RT Per[a]		F2V	Struve (1947)	F1.5V	1.33
		F0V-F1V	Hill et al. (1975)		
CD Tau	F6V		Popper (1971a)	F6V	1.16
HS Hya		F3-F4	Popper (1971a)	F3.5V	1.25
UV Leo	G0V		Popper (1965)	G0V	1.04
	G0V		Hill et al. (1975)		
RZ Cha	F5IV-V		Andersen, Gjerløff (1975)	F5V	1.19
Z Dra[a]		A5	Struve (1947)	F1V	1.35
		2xF4V	Hill et al. (1975)		
AH Vir		K2	Chang (1948)	K1V	0.76
		2xK0-K0III	Hill et al. (1975)		
ZZ Boo	F2		Miner, McNamara (1963)	F2V	1.31
	F2IV-V		McNamara et al. (1971)		
	F2V		Hill et al. (1975)		
BH Vir	G0V		Abt (1965)	F8V	1.09
		4xF8V	Hill et al. (1975)		
DM Vir		F6-F7	Popper (1971a)	F6.5V	1.14
WZ Oph	F8		Popper (1965)	F7.5V	1.11
		F7V	Hill et al. (1975)		
TX Her		A5/A8-F0	Popper (1970)	A8V	1.53
		A9V	Hill et al. (1975)		
FL Lyr[a]		G5	Struve et al. (1950)	G1.5V	1.00
		F8V	Hill et al. (1975)		
V1143 Cyg	F5V		Snowden, Koch (1969)	F5V	1.19
		4xF5V	Hill et al. (1975)		
BS Dra	F5		Popper (1971a)	F5V	1.19
V477 Cyg	A3V		Popper (1968)	A3V	1.86
		A3V	Hill et al. (1975)		
ER Vul	G0V		Northcott, Bakos (1956)	G0V	1.04
EI Cep		F2V/K0III	Hill et al. (1975)	F2V	1.31
EE Peg		A1V	Hill et al. (1975)	A2.5V	1.90
	A4V		Popper (1981)		
CM Lac	A3		Popper (1968)	A2.5V	1.90
		2xA2V	Hill et al. (1975)		
RT And	G0		Payne-Gaposchkin (1946)	F8V	1.09
		F8V	Gordon (1955)		
		F7V	Hill et al. (1975)		
TW And[a]	dF0		Hiltner et al. (1949)	F0V	1.40
		F0V-F2V	Hill et al. (1975)		

[a] Single-lined binary.

to failure of this procedure are small enough not to affect the basic points we shall make. In cases where $B - V$ colors for the individual stars are available or can be calculated (for instance, with XY Cet, EE Peg, CM Lac, and TW And), the color of the primary agrees well with the given spectral type. Masses M_1(Sp.) were next assigned to the primary (hotter) components, based on our assigned spectral types and the empirical spectral type–mass relation given by Habets and Heintze (1981). Single-lined binaries are noted in the tables. The period of each system, the directly measured mass M_1(RV) of the primary star, and the dispersion of the spectrograms from which the radial velocities were obtained are given in Table 2. The second reference, if given, refers to the photometric solution which provides the inclination or mass ratio or both.

Table 3 lists the observed Strömgren indices $b - y$, m_1, and c_1. The given values are either arithmetic means of all values given by an author at various phases (excluding primary eclipse) or mean indices from different sources. In almost every case they refer to the combined light of the components. When there exist published values for the individual components, only those for the primary, hotter component are listed. Data for three systems which have been dereddened (based on the β-index, viz. Crawford 1975, 1979) are so marked. Since there exist β-indices for only three of the detached and semidetached systems, we can calculate tentative reddening corrections for the metallicity index m_1 from $b - y$ color excesses, using the $b - y$ versus spectral type calibration by Rucinski and Kaluzny (1981). However, if we use the same procedure to correct the c_1 indices, several binaries are shifted to "impossible" positions in the $c_1-(b - y)$ diagram. They are displaced from the main-sequence relation in a sense opposite to that for evolved stars and thus lie in a region of the diagram which is normally unoccupied. Also, the inferred color excesses for these stars (up to 0.6 mag) seem too large for their distances of a few hundred parsecs. One can show that this result is due primarily or entirely to their binary nature, to which the observed $b - y$, and thus the predicted standard c_1, are fairly sensitive. Unfortunately, sufficient data do not exist for the full evaluation of these "secondary component reddenings," as we would need reliable four-color light curve solutions for each
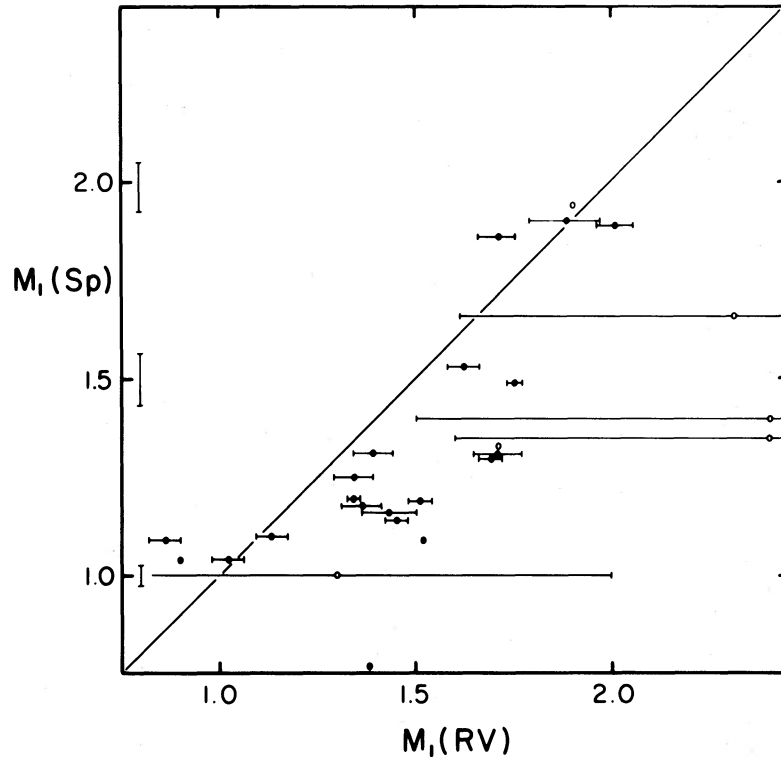
FIG. 1.—Spectral type mass vs. radial velocity mass for main-sequence binary system primaries. *Filled circles*, double-lined; *open circles*, single-lined binaries. Horizontal error bars indicate mean errors of radial velocity mass, as given in the original papers. Vertical bars reflect the spectral type mass shift corresponding to an error of 1.5 spectral subclass in the observed spectral type.

binary. Thus, we have the choice of neglecting reddening corrections in the m_1-index or overcorrecting for reddening by taking the apparent color excesses at face value, even though we know that they result partly from the red secondaries. Accordingly, we have followed both of these extreme courses, with separate diagrams to show the results with and without reddening corrections for the 23 binaries not having β-indices. There is no analogous difficulty for the contact binaries, because the two components have nearly identical temperatures. The contact binary reddening corrections have been taken from the paper by Rucinski and Kaluzny (1981), and all are so corrected.

The quantities $\delta m_1 = m_1(\text{standard relation}) - m_1(\text{system})$ and $\delta c_1 = c_1(\text{system}) - c_1(\text{standard relation})$, where c_1 and m_1 are functions of $b - y$, are given with respect to the standard relations of Rucinski and Kaluzny (1981). This is basically the Hyades relation, as given by Crawford and Perry (1966) for F stars $(b - y < 0.4)$, and an extension to later spectral types which was made by Rucinski and Kaluzny. The $F = [\text{Fe/H}]_{\delta m_1}$ column contains the iron to hydrogen ratios according to the δm_1–[Fe/H] calibration of Appendix A. Clearly it is better to use these m_1-based F values than F values determined directly from curve of growth analyses, even when the latter are available. The large scatter of the directly measured F renders it of little use for our purpose when applied to individual stars, although mean results for large numbers of stars are useful. The last column lists the difference $\delta \log M_1 = \log M_1(\text{RV})$ $- \log M_1(\text{Sp.})$, which is the mass discrepancy of the primary star with respect to the mass expected from its spectral type. The errors in parentheses (if given) are propagated mean errors, assuming an error of ~ 1.5 spectral subclasses. Tables 4, 5, and 6 are similar to the previous ones and show collected

data for contact binaries. Here the adopted spectral types are definitely averages for the two components and need to be corrected for the luminosity transfer through their common convective envelopes, for the effect of rapid rotation on core luminosity, and for the effect of orbital inclination on the system's apparent brightness. The latter two corrections are described in Appendix B. Corrections for luminosity transfer have been made in papers by Mochnacki (1981) and Van Hamme (1982), and we use the same method in this paper. Note that no correction for the change in radius is made in that scheme, although a primary component which becomes detached from its companion will not only increase its (surface) luminosity (it would have to radiate *all* of its core luminosity entirely by itself) but also would increase its radius, and this latter effect must cause a temperature *decrease*. The complete correction for the effective temperature is given by

$$\Delta \log T = \tfrac{1}{4}\Delta \log L - \tfrac{1}{2}\Delta \log R . \qquad (2)$$

The luminosity part of this correction has been applied to each of our contact systems (as in Mochnacki 1981), giving the corrected spectral Sp.", and the corresponding "spectral type mass" $M_1(\text{Sp.''})$, as listed in Table 4. Calculation of the second part of correction (2) would require the computation of a pair of matched stellar structure models for each binary system, which is beyond the scope of this paper. In one case, however, we obtained a quantitative idea of the magnitude of the radius correction. Consider the model contact system computed by Wilson (1978), in which a 1.4 $M_\odot$ primary is in contact with a 0.9 $M_\odot$ secondary. The mean radius of the primary is 1.21 $R_\odot$. Upon computing a model for the primary as a single star (with essentially the same program), we find $R_1 = 1.25 R_\odot$, corresponding to a temperature correction of the order of -100 K.

TABLE 2.

SPECTROSCOPIC AND SPECTROGRAPHIC DATA FOR SELECTED DETACHED AND SEMIDETACHED BINARIES

System	Period (d)	M_1 (R.V.)($M_\odot$)	Dispersion (Å mm⁻¹)	References[b]
X Tri[a]	0.9715	2.3±0.7 (m.e.)	76	Struve (1946) Mezzetti et al. (1980)
RZ Cas[a]	1.1952	1.9	29	Duerbeck, Hänel (1979)
XY Cet	2.7807	1.75±0.02	4x16/14x10.7	Popper (1971b)
TV Cet	9.1033	1.39±0.05	10	Popper (1968) Jørgensen (1979)
RT Per[a]	0.8494	1.7	76	Struve (1947) Mancuso et al. (1977)
CD Tau	3.4351	1.43±0.07	7x10.2/3x10.7	Popper (1971a) Russo et al. (1981)
HS Hya	1.5680	1.34±0.05	13x10.7/3x10.2	Popper (1971a) Giuricin et al. (1980)
UV Leo	0.6001	1.02±0.04	20	Popper (1965)
RZ Cha	2.8321	1.51±0.03	15x20/37x12	Andersen, et. al. (1975) Jørgensen, Gyldenkerne (1975)
Z Dra[a]	1.3574	2.4 ±0.8	76	Struve (1947) Mardirossian et al. (1980)
AH Vir	0.4075	1.38	76	Chang (1948) Binnendijk (1960)
ZZ Boo	4.9917	1.71±0.06	4x10/3x20	Miner, McNamara (1963) Cester et al. (1978)
BH Vir	0.8169	0.86	63	Abt (1965) Giuricin et al. (1980)
IM Vir	4.6694	≥1.45±0.03[c]	14x10.7/2x10.2	Popper (1971a)
WZ Oph	4.1835	1.13±0.04	20	Popper (1965)
TX Her	2.0598	1.62±0.04	10/11	Popper (1970)
FL Lyr[a]	2.1782	1.3 ±0.7	76[d]	Struve et al. (1950) Mardirossian et al. (1980)
V1143 Cyg	7.6408	1.34±0.01	4x8.6/29x13.5-8.9	Snowden, Koch (1969)
BS Dra	3.3640	1.36±0.05	16.1	Popper (1971a) Russo et al. (1981)
V477 Cyg	2.3470	1.71±0.05	visual plates 20 photographic plates 10	Popper (1968)
ER Vul	0.6981	0.90±0.04	20	McLean (1982)
EI Cep	8.4394	1.69±0.03	10.7	Popper (1971a) Cester et al. (1978)
EE Peg	2.6282	2.01±0.06	16	Popper (1981)
CM Lac	1.6047	1.88±0.09	8x10/11x22	Popper (1968) Cester et al. (1978)
RT And[a]	0.6289	1.5	?	Payne-Gaposchkin (1946) Cester et al. (1978)
TW And[a]	4.1227	2.4±0.9	10x76/21x55	Hiltner et al. (1949) Mezzetti et al. (1980)

[a] Single-lined binary.

[b] The second reference, if any, refers to the light curve solution from which the i value was taken.

[c] Value of i unknown.

[d] Assumed according to Struve's generally used dispersion.

This corresponds to less than one spectral subclass and is thus negligible for this one computed case. However, one should remember that the corrections for the luminosity exchange are slight overestimates when the radius effect is neglected.

III. MASS DISCREPANCIES AND METALLICITY: PROCEDURE

In this section we take a closer look at the distribution of the iron to hydrogen ratios for binaries, as a function of the mass discrepancies introduced in § I. The logarithmic iron to hydrogen ratios, [Fe/H], for our sample binaries are plotted versus $\delta \log M_1 = \log M_1(\mathrm{RV}) - \log M_1(\mathrm{Sp.})$ in Figure 2. Error bars, where present, indicate mean errors. They result from the formal propagation of the listed mean errors of the radial velocity masses $M_1(\mathrm{RV})$ and an assumed mean error of 0.02 in $\log M_1(\mathrm{Sp.})$, corresponding to an error of ~ 1.5 spectral subclasses. The plotted error bars are the rms sums of these two independent errors. The same plot with "overcorrections" for interstellar reddening, as discussed in § II, is shown in Figure 3. The plot for contact binaries is shown in Figures 4 and 5. In Figure 4, crosses indicate the uncorrected positions [$M_1(\mathrm{Sp.})$ in Table 4 is used to calculate $\delta \log M_1$.] In Figure 5, crosses mark the positions after corrections have been made for the rotational luminosity drop and for aspect effect. That is, $\delta \log M_1$ is now computed with the value $M_1(\mathrm{Sp.'})$. In each figure the arrows show the shift due to the correction for luminosity transfer. The true positions should be between the heads and tails of the arrows and closer to the heads. Data for the entire set of binaries are plotted in Figure 6. The $\delta \log M_1$ values are listed in Tables 3 and 6.

If our binaries show variation in population type (i.e., metallicity), then we expect the points in Figures 2–6 to slope upward to the right. In fact, such a metallicity effect seems to be present, especially for the contact binaries, although the paucity of stars with very low metallicity renders this conclusion not entirely certain. In overview, we see that the larger and smaller iron to hydrogen ratios correspond to more positive and negative $\delta \log M_1$ values respectively. This is in good qualitative agreement with our expectation from stellar models. The evolutionary stellar models of Mengel et al. (1979) are very useful for testing quantitative agreement. Increasing the metal content of a star of given mass and age decreases its effective temperature, so that a lower temperature (or spectral type) mass $M_1(\mathrm{Sp.})$ would be assigned, and $\delta \log M_1$ would increase. Heavy element content (by mass) Z is related to the

TABLE 3

PHOTOMETRIC DATA AND RELATED PARAMETERS FOR SELECTED DETACHED AND SEMIDETACHED BINARIES

System	$b - y$	m_1	c_1	Reference	δm_1	δc_1	$F = [\mathrm{Fe/H}]_{\delta m_1}$	$\delta \log M_1$ [a]
X Tri	0.184	0.216	0.769	1	−0.030	0.034	0.37	0.143 ± 0.132
RZ Cas	0.063	0.186	0.932[b]	2, 3	0.013	0.000	−0.12	−0.009
XY Cet	0.158	0.220	0.850	3	−0.022	0.050	0.30	0.070 ± 0.021
TV Cet	0.259	0.143	0.540	4	0.027	0.025	−0.14	0.026 ± 0.025
RT Per	0.408	0.143	0.334	3	0.080	0.028	−0.62	0.109
CD Tau	0.315	0.177	0.437	3, 5, 6	−0.001	0.030	0.11	0.091 ± 0.029
HS Hya	0.299	0.147	0.396	7	0.026	−0.034	−0.14	0.030 ± 0.026
UV Leo	0.399	0.197	0.317	3	0.020	0.000	−0.13	$−0.008 \pm 0.026$
RZ Cha	0.309	0.157	0.474	8	0.018	0.057	−0.06	0.103 ± 0.022
Z Dra	0.318	0.175	0.449	3	0.002	0.044	0.09	0.250 ± 0.146
AH Vir	0.464	0.281	0.359[b]	3	0.012	0.108	−0.06	0.259
ZZ Boo	0.250	0.148	0.598	3	0.023	0.058	−0.11	0.116 ± 0.025
BH Vir	0.403	0.148	0.351	3	0.072	0.040	−0.55	−0.103
DM Vir	0.314	0.160	0.500	3	0.016	0.090	−0.04	$\geq 0.105 \pm 0.022$
WZ Oph	0.376	0.119	0.367	3	0.085	0.030	−0.67	0.012 ± 0.025
TX Her	0.178	0.184	0.716	3, 9	0.005	−0.034	0.06	0.025 ± 0.023
FL Lyr	0.363	0.177	0.373	3	0.021	0.023	−0.14	0.114 ± 0.235
V1143 Cyg	0.291	0.168	0.439[b]	3, 9	0.003	−0.006	0.07	0.052 ± 0.021
BS Dra	0.296	0.178	0.431	3	−0.006	−0.004	0.15	0.058 ± 0.026
V477 Cyg	0.087	0.177	0.889	3	0.028	0.004	−0.15	$−0.036 \pm 0.024$
ER Vul	0.391	0.189	0.330	3	0.023	0.005	−0.17	0.008 ± 0.035
EI Cep	0.238	0.142	0.688	3	0.030	0.108	−0.17	0.111 ± 0.021
EE Peg	0.063	0.178	0.975	3	0.021	0.035	−0.09	0.024 ± 0.024
CM Lac	0.109	0.169	0.885	3	0.038	−0.050	−0.24	$−0.005 \pm 0.029$
RT And	0.387	0.173	0.332	3	0.037	0.005	−0.23	0.144
TW And	0.276	0.166	0.745	3	0.004	0.270	0.06	0.234 ± 0.164

[a] $\delta \log M_1 = \log M_1(\mathrm{RV}) - \log M_1(\mathrm{Sp.})$. Mean errors are propagated according to the listed mean error of $M_1(\mathrm{RV})$ and an assumed error of 0.02 in $\log M_1(\mathrm{Sp.})$, corresponding to an error of ~ 1.5 spectral subclasses in the spectral type.

[b] Dereddened according to Crawford 1975, 1979. Data for the other stars are not dereddened.

REFERENCES.—(1) Grønbach 1976. (2) Crawford et al. 1972. (3) Hilditch and Hill 1975. (4) Jørgensen 1979. (5) Perry 1969. (6) Wood 1976. (7) Gyldenkerne et al. 1975. (8) Jørgensen and Gyldenkerne 1975. (9) Hauck and Mermilliod 1980.
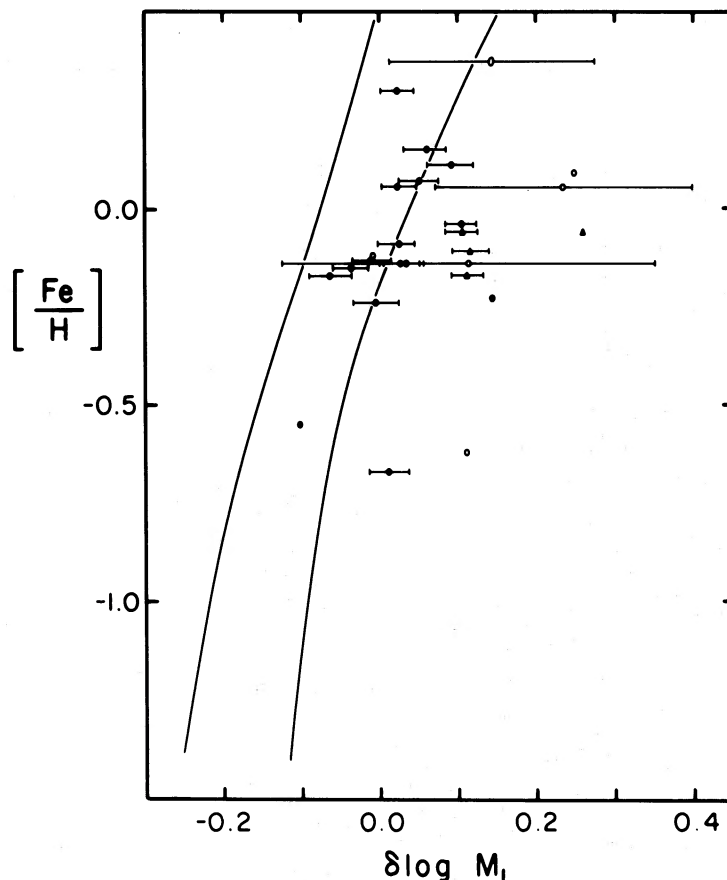

FIG. 2.—Iron to hydrogen ratios [Fe/H] vs. mass discrepancies $\delta \log M_1 = \log M_1(\mathrm{RV}) - \log M_1(\mathrm{Sp.})$ for primaries of detached and semidetached binaries (according to Table 3). *Filled circles*, double-lined; *open circles*, single-lined systems. *Triangles*, double-lined systems with a doubtful luminosity classification. Error bars indicate mean errors, calculated from the mean errors of the radial velocity masses and an assumed mean error of 0.02 in the logarithms of the spectral type masses. The two lines bound the region of expected positions of stars with masses ranging from 0.7 to 2.2 $M_\odot$ and ages between the ZAMS and TAMS.

156

TABLE 4

SPECTRAL TYPE DATA FOR SELECTED CONTACT BINARIES

System	Observed Spectral Type	Reference	Adopted Spectral Type, Sp. Primary	M_1(Sp.)	Corrected Spectral Type, Sp.'[a]	M_1(Sp.')	Corrected Spectral Type, Sp."[b]	M_1(Sp.")
AE Phe	G0 V	1	G0 V	1.04	F9 V	1.06	F4.5 V	1.21
YY Eri	G5	2	G5 V	0.91	G3.5 V	0.95	F7 V	1.12
RZ Tau	F0	3	A8.5 V	1.50	A8 V	1.53	A4.5 V	1.76
	A7 V/A8 V	4						
TX Cnc	G0 V–G1 V	5	G0 V	1.04	F9 V	1.06	F4 V	1.22
	G0 V–G2 V	6						
	F8 V	4						
W UMa	F8	7	F9.5 V	1.05	F7.5 V	1.11	F3.5 V	1.25
	G0	8						
	G0	9						
	2xF8 V/2xG2 V	4						
XY Leo	K0	10	K0 V	0.78	G8.5 V	0.82	G3 V	0.96
	2xK0	4						
CC Com	K6–K7	11	K6.5 V	0.63	K5.5 V	0.66	K3 V	0.72
RZ Com	K0	12	G4 V	0.93	G2 V	0.99	F7 V	1.12
	G0 V/G2 V	4						
44i Boo	G2 V	13	G2 V	0.99	G1 V	1.01	F6 V	1.16
V1010 Oph	A3	14	A4 V	1.79	A3.5 V	1.83	A0 V	2.07
	A5 V	15						
	mid-late A	16						
AK Her	F8	17	F7 V	1.12	F6 V	1.16	F3.5 V	1.25
	F6 V	4						
V566 Oph	F4	18	F3 V	1.27	F2.5 V	1.29	F0 V	1.40
	2xF2 V/F4	4						
ε CrA	F0 V	19	F0 V	1.40	A8.5 V	1.50	A7 V	1.60
VW Cep	G8–K0	20	G9 V	0.80	G7 V	0.85	G0.5 V	1.03
	G8:	4						
V1073 Cyg	A3 V	21	A7 V	1.60	A6.5 V	1.63	A3.5 V	1.83
	F1 V/F2 IV	4						
SW Lac	K0 V	22	G6 V	0.88	G3.5 V	0.95	G0 V	1.04
	G2/G3:	4						
AB And	G5	3	G5 V	0.91	G3 V	0.96	F6.5 V	1.14
	2xG5	4						
U Peg	F3	3	F7.5 V	1.11	F7 V	1.12	F2.5 V	1.29
	G:/G2 V	4						

[a] Corrected only for rotational luminosity drop and aspect.

[b] Corrected for rotational luminosity drop, aspect, and luminosity transfer.

REFERENCES.—(1) Duerbeck 1977. (2) Struve 1947. (3) Struve et al. 1950. (4) Hill et al. 1975. (5) Yamasaki and Kitamura 1972. (6) Whelan et al. 1973. (7) Struve and Horak 1950. (8) Popper 1950. (9) Worden and Whelan 1973. (10) Struve and Zebergs 1959. (11) Rucinski 1976. (12) Struve and Gratton 1948. (13) Popper 1943. (14) Popper 1966. (15) Cowley et al. 1969. (16) Guinan and Koch 1977. (17) Sanford 1934. (18) Heard 1965. (19) Tapia and Whelan 1975. (20) Popper 1948. (21) Fitzgerald 1965. (22) Roman 1956.

TABLE 5

SPECTROSCOPIC AND SPECTROGRAPHIC DATA FOR SELECTED CONTACT BINARIES

System	Period (day)	M_1(RV) ($M_\odot$)	Dispersion (Å mm⁻¹)	References
AE Phe	0.3624	1.37 ± 0.05(m.e.)	20	Duerbeck 1978
YY Eri	0.3215	0.95	76	Huruhata et al. 1953
RZ Tau	0.4157	1.63	76[a]	Struve et al. 1950
TX Cnc	0.3829	1.01 ± 0.09	62	Whelan et al. 1973
W UMa	0.3336	1.20 ± 0.06	62	Worden and Whelan 1973
XY Leo	0.2841	0.58	20	Struve and Zebergs 1959
CC Com	0.2207	0.69 ± 0.06	28	Rucinski et al. 1977
RZ Com	0.3385	1.53	76	Struve and Gratton 1948
44i Boo	0.2678	0.93 ± 0.04	26	Popper 1943
V1010 Oph	0.6614	1.47	42	Margoni et al. 1981
AK Her	0.4215	2.15	75	Sanford 1934
V566 Oph	0.4096	1.18	33	Heard 1965
ε CrA	0.5914	1.12	38	Tapia and Whelan 1975
VW Cep	0.2783	0.78	26	Binnendijk 1967
V1073 Cyg	0.7859	1.29	33	FitzGerald 1965
SW Lac	0.3207	1.13	40	Struve 1949, revised Binnendijk 1970
AB And	0.3319	1.70	76[a]	Struve et al. 1950
U Peg	0.3748	1.22	76[a]	Struve et al. 1950

[a] Assumed according to Struve's generally used dispersion.

157

TABLE 6

PHOTOMETRIC AND RELATED DATA FOR SELECTED CONTACT BINARIES[a]

System	$b - y$	m_1	c_1	Reference	δm_1	δc_1	$F = [\text{Fe/H}]_{\delta m_1}$	$\delta \log M_1$[b]	$\delta \log M_1'$[c]	$\delta \log M_1''$[d]	Mean Error[e]
AE Phe	0.40	0.19	0.32	1	0.03	0.01	−0.23	+0.120	+0.111	+0.054	0.026
YY Eri	0.428	0.208	0.304	2, 3	0.035	0.018	−0.31	+0.019	−0.000	+0.072	...
RZ Tau	0.371	0.109	0.571	2, 3	0.092	0.181	−0.74	+0.036	−0.028	−0.033	...
TX Cnc	0.376	0.208	0.351	2, 3	−0.004	0.014	+0.16	−0.029	−0.021	−0.082	0.044
W UMa	0.415	0.203	0.283	2, 3, 4	0.027	−0.016	−0.14	+0.058	+0.034	−0.018	0.030
XY Leo	0.577	0.403	0.284	2, 3	0.147	0.115	−1.24	−0.129	−0.150	−0.219	...
CC Com	0.759	0.560	0.163	3	0.163	0.081	−1.38	+0.040	+0.019	−0.019	0.043
RZ Com	0.339	0.149	0.294	2, 3	0.036	−0.083	−0.33	+0.215	+0.189	+0.136	...
44i Boo	0.410	0.206	0.292	2, 3	0.019	−0.012	−0.12	−0.027	−0.036	−0.096	0.027
V1010 Oph .	0.127	0.185	0.887	5	0.020	0.005	−0.08	−0.086	−0.095	−0.149	...
AK Her	0.351	0.164	0.392	2	0.027	0.028	−0.15	+0.283	+0.268	+0.236	...
V566 Oph ...	0.271	0.148	0.420	2, 3	0.022	−0.065	−0.10	−0.032	−0.039	−0.074	...
ε CrA	0.247	0.151	0.631	5	0.020	0.078	−0.08	−0.097	−0.127	−0.155	0.172
VW Cep	0.523	0.318	0.266	2, 3	0.104	0.063	−1.14	−0.011	−0.037	−0.121	...
V1073 Cyg ..	0.286	0.156	0.677	2, 3	0.015	0.222	−0.04	−0.094	−0.102	−0.152	0.153
SW Lac	0.478	0.262	0.280	2, 3	0.063	0.042	−0.65	+0.109	+0.075	+0.036	...
AB And	0.511	0.361	0.337	2, 3	0.036	0.125	−0.32	+0.271	+0.248	+0.174	...
U Peg	0.395	0.218	0.334	2, 3	−0.004	0.014	+0.13	+0.041	+0.037	−0.024	...

[a] Dereddened according to Rucinski and Kaluzny 1981.
[b] $\delta \log M_1 = \log M_1(\text{RV}) - \log M_1(\text{Sp.})$.
[c] $\delta \log M_1' = \log M_1(\text{RV}) - \log M_1(\text{Sp.}')$. Contains corrections for rotation and aspect effect.
[d] $\delta \log M_1'' = \log M_1(\text{RV}) - \log M_1(\text{Sp.}'')$. Contains corrections for rotation, aspect, and luminosity transfer.
[e] See Table 3, note a.
References.—(1) Gronbech 1976. (2) Hilditch and Hill 1975. (3) Rucinski and Kaluzny 1981. (4) Linnaluoto and Piirola 1979. (5) Hauck and Mermilliod 1980.
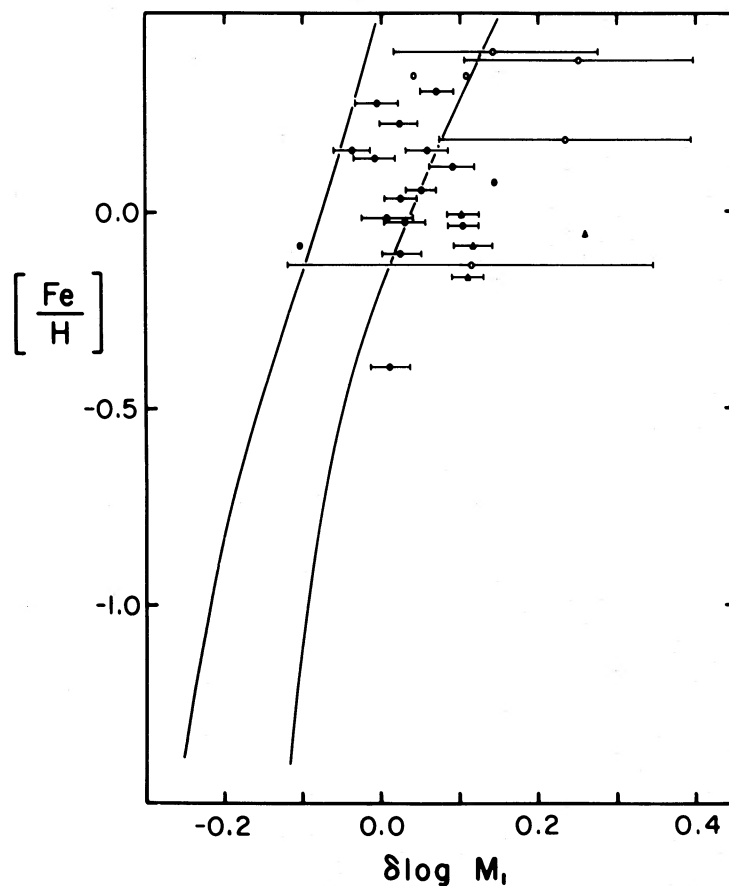

FIG. 3.—Same as Fig. 2, for detached and semidetached systems with "overcorrections" for interstellar reddening
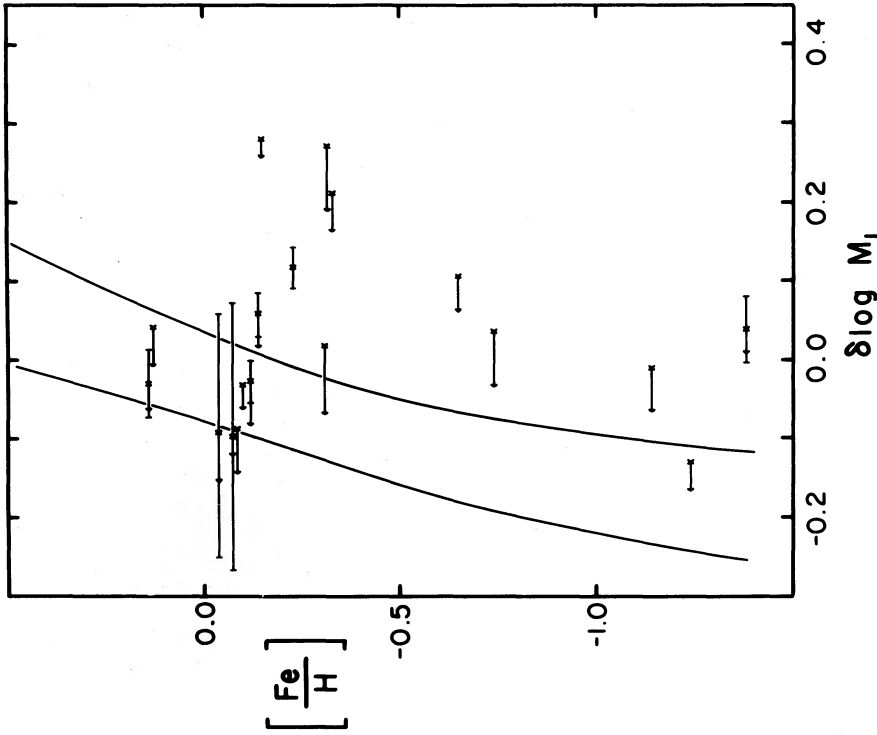
158

Fig. 5

Fig. 4

Fig. 4.—Same as Fig. 2, for contact W UMa-type binaries. *Crosses*, position with no corrections applied. Arrows point to the positions corrected for luminosity transfer. The true position is expected to be between the heads and tails of the arrows, and closer to the heads.
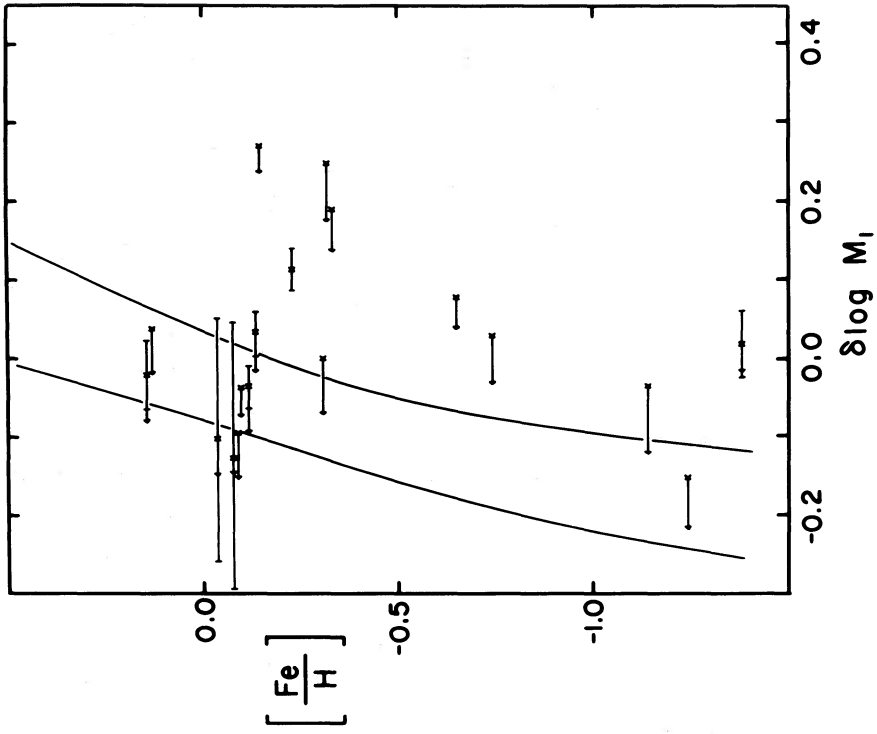Fig. 5.—Same as Fig. 4, with the crosses now indicating the position of W UMa-type primaries, corrected for rotational luminosity drop and aspect
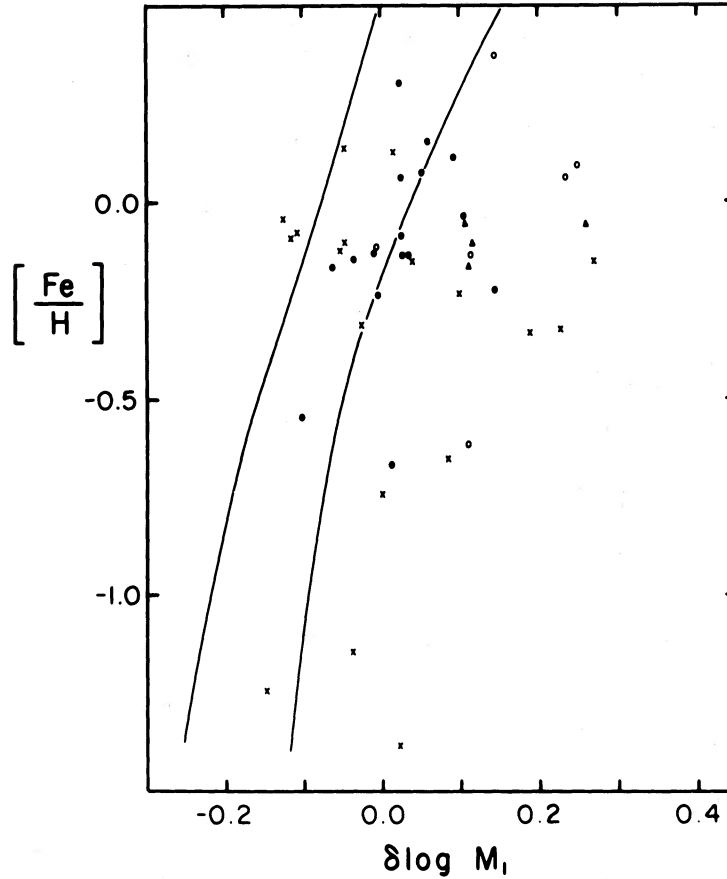
159

FIG. 6.—Combination of Figs. 2 and 4. Crosses, referring to W Uma–type binaries, are the midpoints of the arrows in Fig. 4.

iron to hydrogen ratio (by number of atoms) N_{Fe}/N_H by

$$\frac{1}{Z} = \frac{1.008}{565 N_{Fe} N_H}\left(1 + \frac{Y}{X}\right) + 1 . \qquad (3)$$

The coefficient 565 was calculated with the help of tables in Allen (1973). With the notation $F = [Fe/H]$, we have by definition $F = \log (N_{Fe}/N_H)_* - \log (N_{Fe}/N_H)_\odot$, where subscripts $*$ and $\odot$ refer to a given star and the Sun respectively. We adopt -4.4 for the value of $\log (N_{Fe}/N_H)_\odot$, so that

$$\frac{1}{Z} = \frac{1.008}{565 \times 10^{F-4.4}}\left(1 + \frac{Y}{X}\right) + 1 . \qquad (4)$$

The quantities X and Y are the fractional mass contents of hydrogen and helium respectively, where of course $X + Y + Z = 1$. Stellar models with four different compositions (X, Y, Z) were selected in Mengel et al. (1979). Table 7 lists the F values for these compositions, according to equation

(4). The diagrams of Figures 2–6 are fairly well covered by this choice.

The derivative $dF/d(\delta \log M_1)$ gives a quantitative estimate of the theoretically expected slope in Figures 2–6. The derivative can be written as

$$\frac{dF}{d(\delta \log M_1)} = \frac{dF}{d[\log M_1 - \log M_1(T)]} , \qquad (5)$$

in which M_1 is the true mass of the star and $M_1(T)$ its mass according to the main-sequence temperature—mass relation. Expression (5) can be evaluated by differencing the tables of Mengel et al. (1979). For each Z value, a $(\log T, \log M)$ zero-age main-sequence (ZAMS) relation can be constructed. Then, keeping T_{eff} constant, the change in $\log M$ corresponding to a given change in $\log Z$ (and thus in F) can be obtained by interpolation. Some representative values of expression (5) for low, intermediate, and high masses are listed in Table 8. As the

TABLE 7

CHEMICAL COMPOSITION
AND $F = [Fe/H]$ FOR
THEORETICAL MODELS

Z	Y	X	F
0.001	0.30	0.699	-1.19
0.004	0.30	0.696	-0.59
0.01	0.30	0.690	-0.19
0.04	0.30	0.660	$+0.43$

TABLE 8

THEORETICAL EXPECTED SLOPE IN A $(F, \delta \log M)$–DIAGRAM
FOR SEVERAL MASSES

AVERAGE MASS M	$Z\ 0.001 \rightarrow 0.01$		$Z\ 0.004 \rightarrow 0.04$	
	$d \log M$	$dF/d \log M$	$d \log M$	$dF/d \log M$
0.90	0.072	14.0	0.133	7.7
1.35	0.077	13.1	0.129	7.9
2.00	0.092	10.9	0.161	6.4

theoretically expected slopes of the main-sequence relations in Figures 2–6, these numbers agree with the observed trends within the scatter of the data points. (A simple straight-line fit, without weighting, gives a slope of $dF/d \log M = 12.3 \pm 6.4$ s.d. This slope, although weakly determined, is just in the middle of the range of our theoretical estimates.) However, one would not expect the points in Figures 2–6 to scatter closely about a line with slope given by Table 8, because the slope is only approximately constant (i.e., because the real relation will be somewhat curved and because the main-sequence relation which includes all luminosity class V stars will have a substantial width). Thus the numbers in Table 8 are intended only as roughly characteristic of the δ mass—composition main sequence. The actual main-sequence bands in Figures 2–6 were constructed accurately, by means of the abovementioned ($\log T$, $\log M$)–relations from Mengel et al. (1979). Starting from input values of M_1 and [Fe/H], we converted [Fe/H] to Z through relation (4). The Mengel et al. ZAMS ($\log T$, $\log M$)–relations then provide (again, with interpolation) $T_{\rm eff}$ and thus the spectral type. From the Habets and Heintze relation between spectral type and mass we then find $M_1(\rm Sp.)$. Differencing the input (true) mass and the output (spectral type) mass, we finally find the horizontal coordinate for a point on a ZAMS relation for Figures 2–6. The vertical coordinate, of course, is the input [Fe/H] value. We repeated this procedure over a range of [Fe/H], so as to find a curve in each of Figures 2–6. Repeating the entire procedure over a range of input masses from 0.7 to 2.2 $M_\odot$, we find a family of such curves, whose envelope defines an area in each of Figures 2–6. We next repeated all of the foregoing for stars on the terminal-age main sequence (TAMS) of Mengel et al. and again for stars midway between the ZAMS and TAMS.[2] We now have areas in Figures 2–6 which are the loci of all ([Fe/H], $\log M$)–relations included within a range of mass and main-sequence evolution. One must be very careful in thinking of the meaning of this area, because the two broadening effects (in mass and in evolution) interact in a complicated way. For example, one cannot simply think of the left side as representing the least evolved stars, because low-mass stars become hotter (bluer) in their initial evolution from the ZAMS, and thus begin moving from right to left–not left to right—in the diagram. Of course, post–main-sequence evolution causes motion to the right for stars of all masses. One should think of the main-sequence areas in these plots only as regions which should contain the points for all stars which have evolved no further than the TAMS.

Observationally, however, the points scatter not within the main-sequence area, but about its right border, with many points lying well outside to the right, where only stars in post–main-sequence evolution should be found. This effect cannot result from the particular $M(\rm Sp.)$ calibration which we used, because use of a different calibration would cause equal horizontal shifts in both the points and the curves which define the main-sequence band. Thus the relative positions of the points with respect to the bands (Figs. 2–6) are essentially independent of the adopted $M(\rm Sp.)$ calibration. So we are faced with the fact that a considerable fraction of our supposedly main sequence primary stars appear to have evolved beyond core hydrogen burning—in contradiction to their luminosity classes. However, before drawing any conclusions from this, we

next investigate the correlation of our mass discrepancies with spectrographic dispersion.

IV. MASS DISCREPANCIES AND METALLICITY: RESULTS

The observed mass discrepancies (§ III) show the expected metallicity and age effects, but in many cases by amounts which are characteristic of post–main-sequence stars. However, because of the luminosity class V selection criterion, one might feel uncomfortable with a post–main-sequence explanation. Of course, the Mengel et al. (1979) models could be responsible, but that seems unlikely because the MAMS $M(\rm Sp.)$ relation (theoretical) for these models differs only slightly (~ 0.015 in $\log M$) from the empirical Habets and Heintze relation. Let us therefore consider other possibilities. It is now time to address two of our main questions: can systematic radial velocity measurement errors be demonstrated to exist, and are they a principal cause of the effects we have seen? Since all the binaries selected for our tables have observed metallicity indices on the Strömgren system, we are in a position to predict their mass discrepancies, $\delta \log M_1$. Thus we can form a quantity $\Delta = \delta \log M_1$(observed) $- \delta \log M_1$(theoretical, MAMS), which is the excess mass discrepancy after correction for metallicity. Unfortunately, we have no analogous way to correct for the (unknown) evolutionary state, but at least our quantity Δ is free of disturbing effects as one can make it. We now plot Δ as a function of the spectrographic dispersion used in determining the radial velocity masses. Figures 7 and 8 show the results for detached and semidetached binaries, while Figure 9 does the same for contact binaries. The upper and lower horizontal lines represent the borders of the main-sequence band. The arrows attached to the contact binary points have the same meaning as in Figures 4–5. For the detached and semidetached binaries at lowest dispersion, we do see a systematic shift of the (very uncertain) points in the sense of measured (radial velocity) mass being larger than temperature (spectral type) mass. We are not convinced, however, that this shift is primarily due to systematic errors of measurement and shall argue at a later point that it is likely to be due to an observer-dependent selection effect. Figures 7 and 8 also show an upward shift of the detached and semidetached binaries even at high dispersion, but not by so great an amount as at low dispersion. We think that another selection effect may operate here, and we discuss it later, along with the first effect. For the contact binaries we see little dependence on dispersion, except at the very lowest dispersions. Here (in Fig. 9) one must be careful to look at the heads of the arrows (corrected for luminosity transfer) rather than at the crosses. Also, the shift upward with respect to the main-sequence band is not so obvious, although several points do lie in the post–main-sequence region, which is a very perplexing situation for W UMa–type stars.

The overall situation shown by Figures 7–9 is that no gradual trend of mass anomalies with dispersion is apparent, but there are excess anomalous mass determinations (for detached, semidetached, and contact systems) at the lowest dispersions. The largest of these are of the order of a factor of 2. Possible causes of this effect, and of the existence of data points which lie to the evolved side of the main-sequence band, are suggested in the next section.

V. RESIDUAL ANOMALIES

We now consider possible explanations for the general upward shift of points in Figures 7–9 and for the enhanced effect at the lowest dispersions. First we ask if the shift could be

---

[2] The terminal-age main-sequence (TAMS) and mid-age main-sequence (MAMS) models from Mengel et al. were taken to be those with $\log g$ values of 0.50 and 0.25 respectively, smaller than those of the ZAMS models.
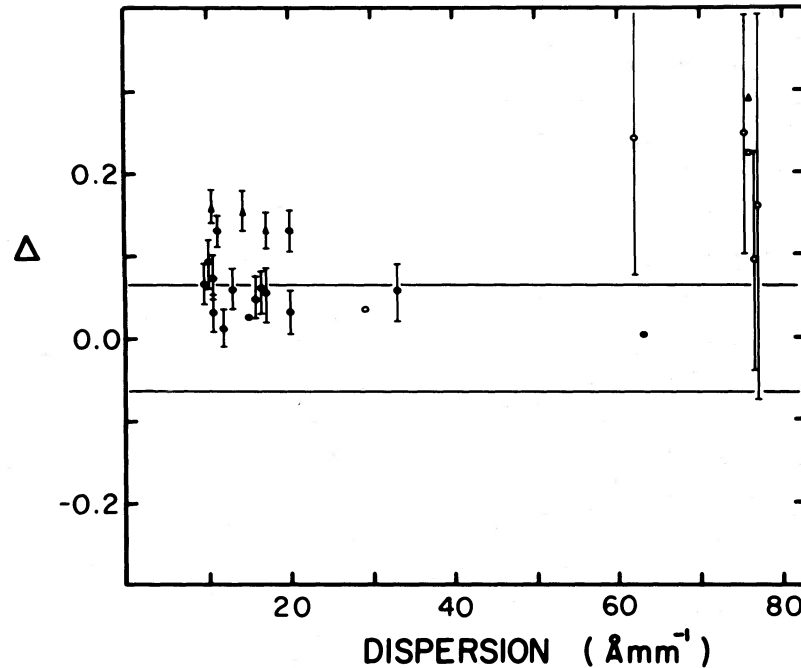
FIG. 7.—Difference $\Delta = \delta \log M_1$(obs.) $- \delta \log M_1$(theoretical, MAMS) of the observed mass discrepancy and the theoretically expected one, given the mass, chemical composition, and a MAMS age, vs. spectrographic dispersion of the plates from which radial velocities were measured. Symbols have the same meaning as in previous figures. This figure is for detached and semidetached systems.

due to incorrect luminosity classifications. The possibility that this may be the case for at least some of the detached and semidetached binaries is suggested by the fact that four of them have been estimated to be class IV or even class III by one observer (these are marked by triangles in Figs. 2, 3, 6, 7, and 8). However, we have inspected the measured (radial velocity) radii for all these stars, and none exceed the radii expected for TAMS stars. Straightforward interpretation of the evidence

therefore indicates that all or virtually all the stars are indeed of luminosity class V. Another problem which we need to understand is why no points are found near the lower boundary of the main-sequence band of Figure 7 (detached and semidetached binaries). Certainly there is a significant selection effect by which binaries with evolved (i.e., enlarged) components have an increased probability of showing eclipses and thus being included in our sample. This effect has been investi-
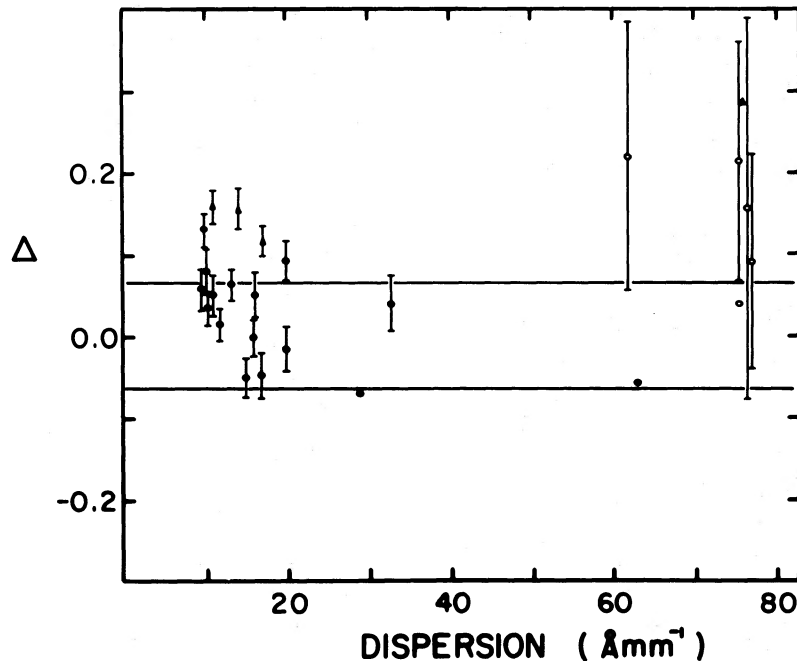
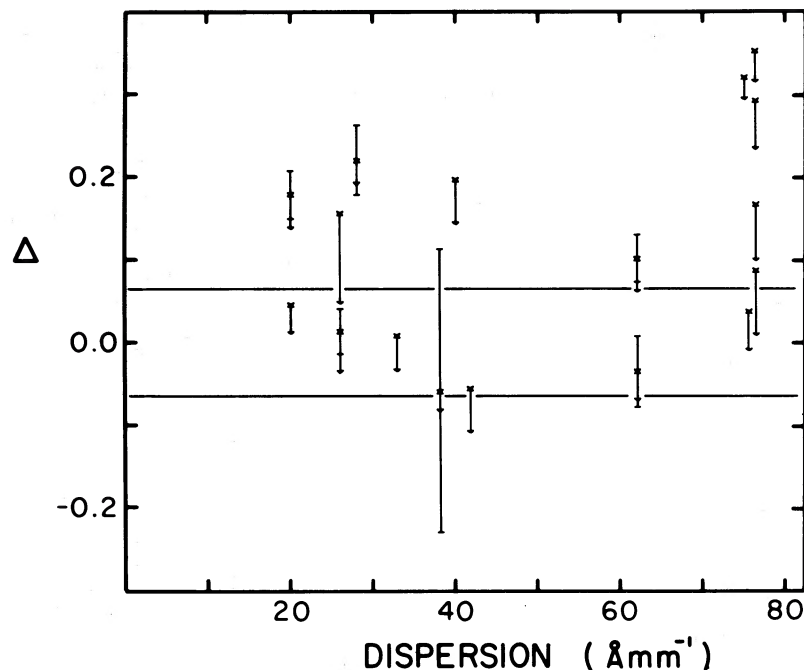FIG. 8.—Same as Fig. 7, with "overcorrection" for interstellar reddening

Fig. 9.—Same as Fig. 7, but for W UMa–type binaries

gated by Morgan and Eggleton (1979) in the context of the RS CVn phenomenon, and it may indeed be responsible for the apparent lack of binaries which are little evolved. Considering now the contact binaries, one could not very well suggest that some are class IV or III stars because they are all W UMa–type stars and are constrained by their short periods to be main-sequence systems. The data points for these stars have been corrected for luminosity exchange and two kinds of (uniform) rotational effects, and we have verified that several other effects are negligible. The only possibly important effect we can think of which has not been evaluated is *differential* rotation. Large drops in luminosity and effective temperature are caused by fast core rotation (Faulkner, Roxburgh, and Strittmatter 1968; Law 1981), and we could indeed have an opportunity here to identify stars with fast-spinning cores. While the idea is most attractive for the contact binaries, where no other suggestion seems available, it could also be important for the detached and semidetached systems.

We reserve for last a selection effect which is nearly impossible to quantify but which we strongly suspect to be significant. Published radial velocity curves for the lowest dispersion cases have not only large scatter but typically only small numbers of observations (say 15–20, with as few as four in one instance!). Consider the practical effect of these circumstances. Because of the collective effect of random errors, we see curves which in some cases bear little resemblance to the expected sine curves. In particular note that when the individual residuals "conspire" to increase the amplitude, we should still have a recognizable binary velocity curve, but when the opposite occurs we can expect a rather disheveled collection of points which an observer would be relatively unlikely to bother analyzing or publishing. Thus even purely random errors can give rise to a situation in which lower amplitude (lower mass) results are systematically suppressed, leading to a statistical bias in measured masses. We call this the NP (nonpublication) effect. Actually there would be two related effects, which might be called NP1 and NP2. The first is illustrated by a hypothetical set of many velocity curves for the same binary. The effect is

that those which show smaller amplitudes would be relatively unlikely to be published. The second effect is that for a set of binaries distributed over a range of total mass, the results for those with the smaller masses will tend not to be published, for the same reason as in the first effect. One must realize, of course, that a distribution in mass translates into a distribution in $T_{\rm eff}$ which will mimic that caused by the width of the main-sequence band. While the quantification of this idea is a problem in experimental psychology, we can at least demonstrate its plausibility by generating a number of simulated "observed" curves with randomly perturbed velocity points. Figure 10 displays 20 simulated velocity curves, each of which has 15 points at the same set of phases—the phases observed for AK Her by Sanford (1934). The "velocities" are points on a sine curve to which normally distributed random errors have been added. The standard deviation was chosen to be representative of that seen in actual very low dispersion velocity curves, and is 0.25 times the semiamplitude of the unperturbed curve. Inspection of Figure 10 suggests that some of these curves (mainly the ones with smaller amplitudes) would be far less likely to be analyzed and published than certain others.

Some persons might object that it makes little practical difference whether the anomalous masses determined at low dispersion result from systematic observational errors or from a selection effect, but the distinction is an important one. If systematic errors are involved, a given observer currently can do nothing to cope with the situation because the nature of the supposed errors is not at all understood. The appropriate course of action would then be to refrain from observing with low-dispersion equipment—the only kind available at many observatories. However, if the NP selection effect is the only opponent, then the observational errors are random, and an obvious remedy is simply to make larger numbers of observations for each binary, since the effects of random errors can always be overcome by improving the number statistics. Since the number of data points in typical published velocity curves is astonishingly small (fewer than 10 is not unusual), an avenue could be open for observers with modest equipment to
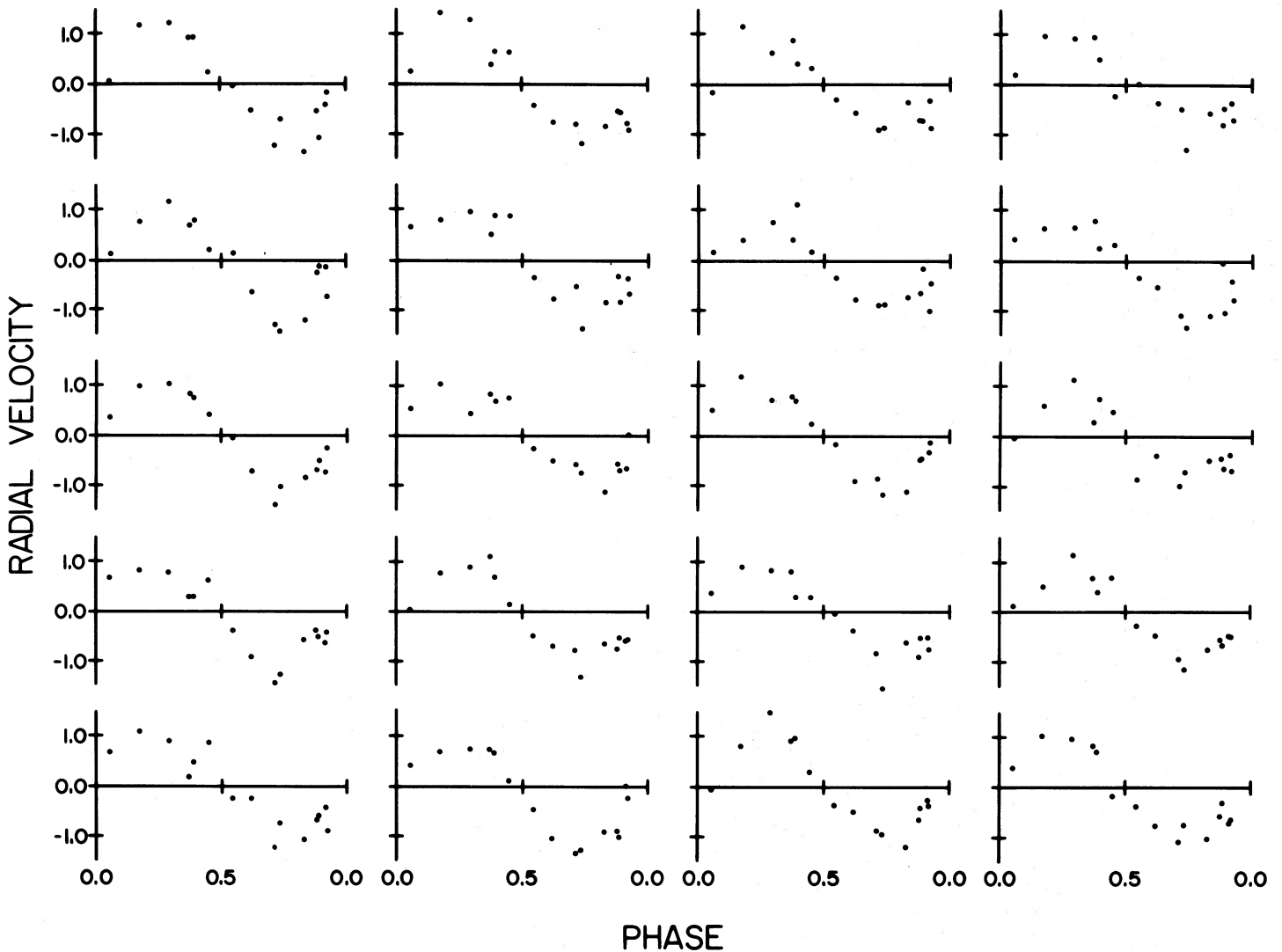
FIG. 10.—Simulated radial velocity curves. The scatter is random, so that no mass bias should occur if all curves are analyzed and published. However, a bias toward larger masses will be found if the lower amplitude curves are not published, as seems likely.

make major contributions to binary star mass data—provided they are willing to gather velocity curves with 50–100 observations.

In conclusion, our figures show the expected dependence of mass discrepancies on chemical composition and three additional effects which require explanation. The lack of stars near the ZAMS boundaries of our mass discrepancy diagrams is probably due to an observational selection effect by which unevolved stars are relatively unlikely to show eclipses. The enhanced mass discrepancies at lowest dispersion might be caused by systematic radial velocity measurement errors, as commonly believed, but we think that the NP selection effect is

at least as likely to be responsible. Potentially most interesting is the possibility that the third effect—mass discrepancies which are too large to be explained by main-sequence evolution and which are found even for high spectroscopic dispersion—may be the first observational evidence for strong differential rotation in normal binaries.

APPENDIX A

CALIBRATION OF THE IRON TO HYDROGEN RATIO [Fe/H] WITH THE METALLICITY INDEX m_1

Since no [Fe/H]–δm_1 calibration has been made for stars of late spectral type and many more data are now available, we have made a new calibration.[3] The parameter δm_1 is usually defined as the difference m_1(standard relation) $- m_1$(observed), for a given

[3] Another new [Fe/H] vs. δm_1 calibration (for early G stars) has just been published by McNamara and Powell (1985). Use of this calibration would not significantly change our conclusions.

TABLE 9
DATA FOR THE [Fe/H]–δm_1 CALIBRATION

Star (HD number)	Spectral type	[Fe/H]	b-y	m_1	δm_1	Star (HD number)	Spectral type	[Fe/H]	b-y	m_1	δm_1
F-stars								-0.32			
5015	F8V	0.06	0.346	0.193	0.008	32923	G4V	-0.20	0.415	0.197	0.033
9826	F8V	-0.23	0.344	0.179	0.008	34411	G0V	0.22	0.389	0.206	0.005
		-0.11				39587	G0V	0.25	0.378	0.194	0.011
		-0.14						-0.12			
22484	F9V	0.37	0.368	0.174	0.022	48682	G0V	0.15	0.357	0.185	0.009
		-0.16				52711	G4V	-0.15	0.374	0.198	0.005
		-0.12				55575	G0V	-0.21	0.370	0.173	0.028
30562	F8V	0.13	0.396	0.209	-0.005			-0.44			
30652	F6V	0.16	0.298	0.164	0.009	63077	G0V	-0.98	0.373	0.132	0.070
32537	F0V	0.10	0.217	0.152	0.025			-0.8			
33256	F2V	-0.60	0.300	0.145	0.035			-0.82			
38393	F6V	-0.07	0.317	0.154	0.032			-0.90			
69897	F6V	-0.52	0.314	0.146	0.036			-0.70			
76932	F6V	-1.1	0.362	0.123	0.122	72905	G1.5V	-0.27	0.390	0.206	0.005
88218	F8V	-0.42	0.386	0.186	0.039	84737	G2V	-0.04	0.390	0.203	0.008
90277	F0V	0.20	0.151	0.195	-0.002	86728	G4V	0.34	0.416	0.234	-0.004
90839	F8V	-0.23	0.341	0.172	0.024			0.34			
91324	F6V	-0.60	0.326	0.141	0.060			-0.08			
102634	F7V	0.14	0.327	0.181	-0.004			0.03			
		0.10				90508	G1V	-0.23	0.396	0.180	0.035
102870	F8V	0.33	0.354	0.187	0.000			-0.23			
		0.26				95128	G0V	-0.02	0.392	0.203	0.009
		0.28				102365	G5V	-0.48	0.408	0.209	0.013
		0.15						-0.70			
		0.19				109358	G0V	0.02	0.385	0.182	0.032
		0.29						0.08			
106516	F5V	0.05	0.319	0.115	0.083			-0.23			
		-0.86				110897	G0V	-0.32	0.372	0.153	0.049
		-0.40						-0.30			
		-0.65						-0.47			
110379	F0V	-0.57	0.244	0.150	0.021	114710	G0V	0.19	0.370	0.191	0.010
114762	F9V	-0.59	0.360	0.144	0.067			0.08			
115383	F8V	0.10	0.376	0.191	0.023			0.05			
120136	F7V	0.28	0.319	0.438	-0.006			0.27			
		0.14						0.16			
128167	F3V	-0.20	0.253	0.132	0.038			0.18			
		-0.42				115043	G1V	-0.34	0.388	0.197	0.013
142373	F9V	-0.40	0.380	0.158	0.053			-0.06			
		-0.29				117176	G5V	-0.11	0.446	0.232	0.035
		-0.35				136352	G2V	-0.52	0.398	0.182	0.034
142860	F6V	-0.40	0.319	0.151	0.032			-0.46			
		-0.07				141004	G0V	-0.04	0.385	0.199	0.009
		-0.11						0.15			
148816	F8V	-0.54	0.361	0.127	0.079			-0.02			
157089	F9V	-0.57	0.374	0.152	0.046	143761	G2V	-0.20	0.394	0.183	0.031
		-0.54						-0.17			
		-0.52						-0.14			
165908	F7V	-0.51	0.357	0.137	0.066	146233	G1V	0.02	0.397	0.221	0.033
		-0.45				152792	G0V	-0.45	0.408	0.198	0.024
		-0.39						-0.31			
		-0.42				157214	G0V	-0.36	0.409	0.182	0.042
		-0.53						-0.58			
170153	F7V	-0.33	0.331	0.146	0.056			-0.34			
185395	F4V	0.04	0.261	0.158	0.012	186408	G2V	0.22	0.410	0.214	0.011
203608	F6V	-0.67	0.321	0.124	0.079			0.20			
		-0.7				186427	G5V	0.11	0.416	0.226	0.004
210027	F5V	-0.10	0.296	0.159	0.011			0.07			
215648	F7V	-0.05	0.330	0.147	0.042	187923	G0V	0.00	0.424	0.190	0.048
218470	F5V	-0.31	0.286	0.152	0.018			0.12			
222368	F7V	-0.51	0.329	0.164	0.029	189567	G2V	-0.28	0.397	0.200	0.016
		0.09				208776	G0V	-0.26	0.382	0.169	0.038
						217014	G5V	0.12	0.416	0.232	-0.002
G-stars						224930	G3V	-0.55	0.428	0.189	0.054
								-0.70			
1461	G0V	0.43	0.419	0.243	-0.010			-0.60			
3443	G8V	-0.16	0.427	0.254	-0.011			-0.59			
4614	G0V	-0.17	0.372	0.185	0.017			-1.08			
10307	G2V	0.20	0.389	0.203	0.008			-0.52			
		-0.03									
		0.16				**K-stars**					
		0.14									
13974	G0V	-0.43	0.386	0.191	0.018	3651	K0V	-0.06	0.509	0.377	0.015
20766	G2V	-0.37	0.404	0.203	0.018	25329	K1V	-1.32	0.528	0.299	0.136
		-0.10						-1.34			
20794	G8V	-0.34	0.426	0.222	0.018	26965	K1V	-0.19	0.488	0.322	0.008
20807	G1V	-0.04	0.381	0.183	0.023			0.01			

VAN HAMME AND WILSON

TABLE 9—*Continued*

Star (HD number)	Spectral type	[Fe/H]	b-y	m_1	δm_1	Star (HD number)	Spectral type	[Fe/H]	b-y	m_1	δm_1
149661	K2V	0.01	0.489	0.352	0.000			-0.05			
166620	K2V	-0.20	0.523	0.412	0.010			-0.15			
		-0.30						-0.10			
185144	K0V	-0.23	0.472	0.320	-0.010	219134	K3V	0.00	0.580	0.551	0.004
		-0.25						0.10			
191408	K3V	-0.03	0.518	0.326	0.084			0.00			
201091	K5V	0.00	0.656	0.677	-0.022			-0.21			
		-0.05						0.00			
		-0.10						-0.01			
		-0.06						0.20			
201092	K7V	-0.65	0.791	0.676	0.051						

NOTE.—All iron to hydrogen ratios are taken with respect to the Sun as reference star.

value of a temperature indicator. This can be the $b - y$ color index or the Hβ line strength index β, with the latter having the advantage of being independent of interstellar reddening. However, β loses its dependence on effective temperature for G and later type stars, so to extend the existent F-star calibration to later spectral types, $b - y$ must be the independent variable.

The standard relation with respect to which the δm_1 values were calculated is that of Rucinski and Kaluzny (1981). For $b - y < 0.4$, this relation is basically that of the Hyades cluster, as determined by Crawford and Perry (1966). The extension to cooler stars was made by Rucinski and Kaluzny, and we refer to their paper for discussion of this relation.

The relative iron to hydrogen ratio [Fe/H] of a star with respect to some reference star (often the Sun) is [Fe/H](star) − [Fe/H](reference star). The abundance ratios are in numbers of atoms, and a simple procedure (see § III) allows transformation of this ratio to Z, the heavy element content by mass fraction. The material for constructing a [Fe/H]–δm_1 calibration was taken from a recent version of the catalog of [Fe/H] determinations of Cayrel de Strobel *et al.* (1980) and the *uvbyβ Photoelectric Photometric Catalogue* of Hauck and Mermilliod (1980). Stars in the spectral type range F–K with luminosity class V and Strömgren indices have been selected and are listed in Table 9. A general plot of all [Fe/H] versus δm_1 data shows a linear relationship with slightly different slopes for F, G, and K stars. A linear calibration of the form [Fe/H] $= a + b\delta m_1$ was carried out for each spectral range. The intercept a and slope b were estimated by least squares and are given in Table 10, and this calibration is shown in Figure 11.

Crawford (1975), using data compiled by Cayrel and Cayrel de Strobel (1966), gives for F stars the relation [Fe/H] $= 0.3 - 12.5\delta m_1$. Nissen (1970) obtained [Fe/H] $= 0.41 - 12.7\delta m_1$ for F5–G2 main-sequence stars, and Gustafsson and Nissen (1972) found a relation [Fe/H] $= 0.40 - 15\delta m_1$ for F1–F2 stars. Our F-star calibration has a somewhat smaller slope and intercept, but since a slightly different standard relation for calculating δm_1 values has been used in each case, these differences are not considered significant. Our calibration implies a Hyades relative iron to hydrogen measure F of ~ 0.11.

APPENDIX B

TEMPERATURE CORRECTIONS FOR ROTATIONAL LUMINOSITY REDUCTION AND FOR ASPECT

Structural models for uniformly rotating stars have been computed in several papers, for example by Faulkner, Roxburgh, and Strittmatter (1968). For differentially rotating stars, Bodenheimer (1971) has shown that although luminosity depends strongly on total rotational angular momentum J, it depends only slightly on the internal distribution of J. Therefore one can approximate the rotational luminosity loss as a function of mass M and J alone. We use the relation

$$\Delta \log L = -1.37 \times 10^{31} J^2/M^4 , \tag{B1}$$

which we found to fit the results given by Law (1981) in her Figure 8. We have applied this correction to the log L values for (the primary components of) our contact binaries so as to obtain the luminosities for nonrotating stars, on the assumption of *uniform* rotation. The rotational luminosity change is typically of the order of 7%. It is convenient to use an expression for Δ log L in terms

TABLE 10

THE [Fe/H] VERSUS δm_1 CALIBRATION

Spectral Range	Number of Stars	a	b	σ
F	61	$+0.10 \pm 0.04$	-9.05 ± 0.9	0.20
G	81	$+0.11 \pm 0.04$	-12.0 ± 1.2	0.22
K	26	-0.06 ± 0.05	-6.6 ± 1.1	0.24
F + G + K	168	$+0.04 \pm 0.02$	-8.7 ± 0.6	0.22

NOTE.—The intercept a and slope b are listed with their mean error. σ is the standard deviation of the linear fit.
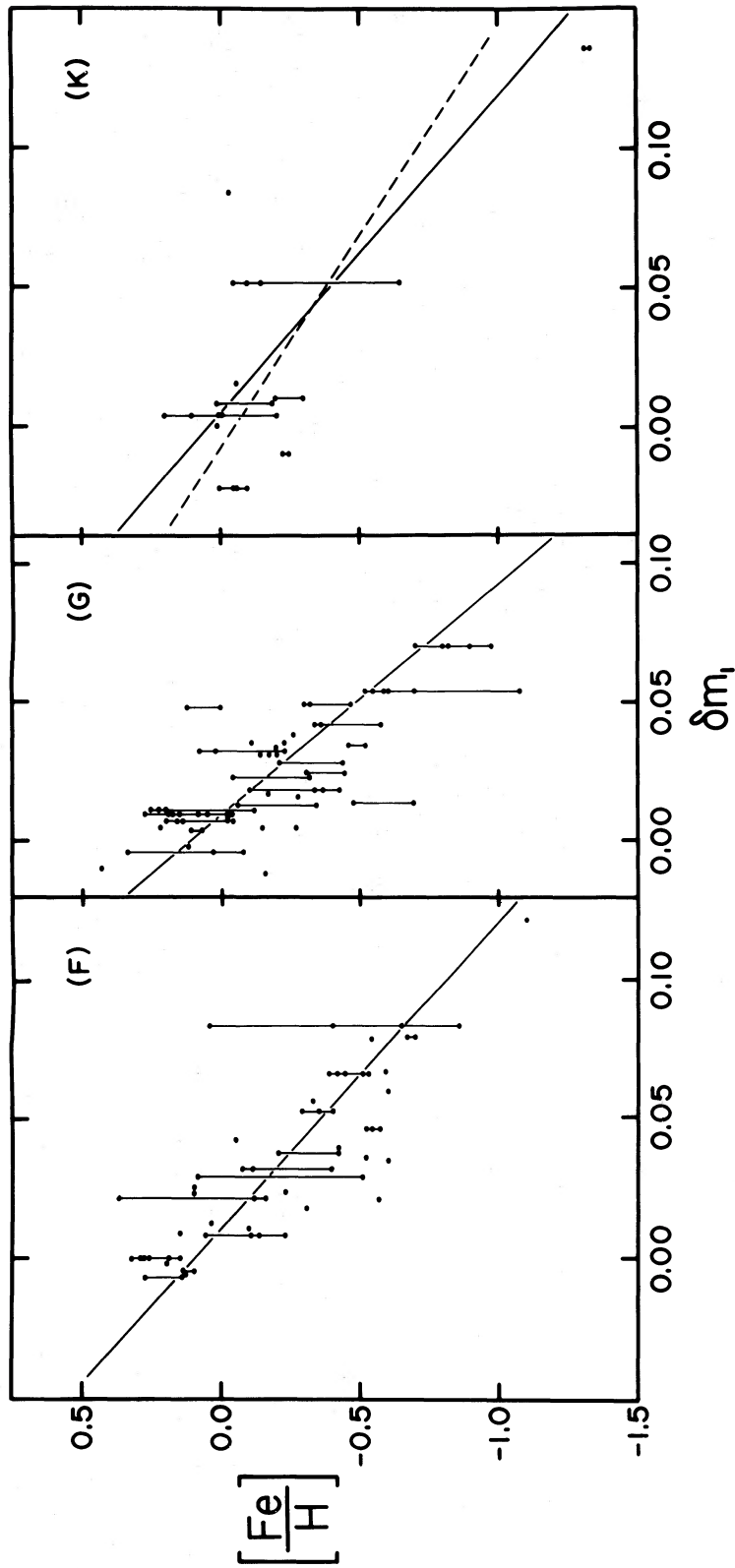
FIG. 11.—[Fe/H] vs. δm_1 calibration of Appendix A. Vertical bars connect different [Fe/H] measurements for the same star. For the K stars, the dashed line represents the linear least-squares fit, while the solid line represents the fit to the complete set for F, G, and K stars.

of more directly measured quantities, for which we use

$$\Delta \log L = 0.43 \left(\frac{k^2 R_1^{\,2}}{M_1 P} \right)^2 . \tag{B2}$$

Here k is the moment of inertia appropriate to a main-sequence star (in units of its radius) and has been taken from Table 4 of Van Hamme (1982). The primary's radius, mass, and orbital period are denoted by R_1, M_1, and P, and are in solar radii, solar masses, and days respectively. The luminosity will then be in ergs s^{-1}. The radii can be found conveniently from

$$R_1 = r_1 [74.4 M_1 (1 + q) P^2]^{1/3} , \tag{B3}$$

where the dimensionless quantities r_1 and q are the relative radius (unit = orbital semimajor axis) and the mass ratio. Finally, the temperature correction is given by equation (B2) and the first term of equation (2).

To correct for the aspect effect, we assume blackbody radiation and assign a "mean Planck factor" $P(i)$, which is averaged over the visible surface and is a function of orbital inclination. The factor $P(i)$ is a surface brightness and scales with the received flux per unit visible area on the primary star.

$$P(i) = C_1 \frac{F(i)}{A(i)} . \tag{B4}$$

We can easily compute the monchromatic flux $F(i)$ with a binary star light curve program, but the *apparent* area $A(i)$ is not routinely produced by such a program. However, $F(i, 0, 0)$, the $F(i)$ value for zero limb and gravity darkening, *is* directly obtained from such a program and is proportional to the apparent area (i.e., subtended solid angle) of the star. Thus, inserting another scaling factor C_2, we can write

$$P(i) = C_2 \frac{F(i, x, g)}{F(i, 0, 0)} , \tag{B5}$$

which directly expresses the fact that $P(i)$ is nonconstant only because of limb and gravity darkening. Of course, we must select some definite wavelength, for which we chose 4400 Å. Allowing C_2 to be a free parameter, we find a family of curves $P(i)$ or, since T is a unique function of P, we have a family of curves $T(i)$. For only one value of C_2 will the $T(i)$ curve pass through the point (T_{observed}, i_{observed}) for a given binary. Having now determined C_2, we have a definite function $T(i)$ for the primary star of each binary. We now adopt, as the appropriate mean effective temperature (averaged over inclination), the mean of all temperatures which would be seen by an ensemble of observers distributed uniformly over a large sphere concentric with the star. The mean is given by

$$T_m = \int_0^{\pi/2} T(i) \sin i \, di . \tag{B6}$$

There will be some inclination i_m for which $T(i_m) = T_m$, and while i_m is not exactly the same for all binaries, we find that it is very nearly the same, 55° ± 1°, for all cases we have checked. Thus for a binary with $i = i_m$, $T_m = T_{\text{observed}}$, while for all our tabulated binaries $T_m > T_{\text{observed}}$, and the difference $T_m - T_{\text{observed}}$ can readily be found from a suitable graph. These corrections have been found and applied for all our binaries. They have corrected spectral types Sp.′ and corresponding spectral type masses M_1(Sp.′), as listed in Table 4.

REFERENCES

Abt, H. A. 1965, *Pub. A.S.P.*, **77**, 367.
Allen, C. W. 1973, *Astrophysical Quantities* (3d ed.; London: Athlone).
Andersen, J., Gjerløff, H., and Imbert, M. 1975, *Astr. Ap.*, **44**, 349.
Binnendijk, L. 1960, *A.J.*, **65**, 358.
———. 1967, *Pub. Dominion Ap. Obs.*, **13**, 27.
———. 1970, *Vistas Astr.*, **12**, 217.
Bodenheimer, P. 1971, *Ap. J.*, **167**, 153.
Cayrel, R., and Cayrel de Strobel, G. 1966, *Ann. Rev. Astr. Ap.*, **4**, 1.
Cayrel de Strobel, G., Bentolila, C., Hauck, B., and Curchod, A. 1980, *Astr. Ap. Suppl.*, **41**, 405.
Cester, B., Fedel, B., Giuricin, G., Mardirossian, F., and Mezzetti, M., 1978. *Astr. Ap. Suppl.* **32**, 351.
Cester, B., Giuricin, G., Mardirossian, F., and Mezzetti, M. 1978, *Astr. Ap. Suppl.*, **32**, 347.
Chang, Y. C. 1948, *Ap. J.*, **107**, 96.
Cowley, A., Cowley, C., Jaschek, M., and Jaschek, C. 1969, *A.J.*, **74**, 375.
Crawford, D. L. 1975, *A.J.*, **80**, 955.
———. 1979, *A.J.*, **84**, 1858.
Crawford, D. L., Barnes, J. V., Gibson, J., Golson, J. C., Perry, C. L., and Crawford, M. L. 1972, *Astr. Ap. Suppl.* **5**, 109.
Crawford, D. L., and Perry, C. L. 1966, *A.J.* **71**, 206.
Duerbeck, H. W. 1977, *Acta Astr.* **27**, 51.
———. 1978, *Acta Astr.*, **28**, 49.
Duerbeck, H. W., and Hänel, A. 1979, *Astr. Ap. Suppl.*, **38**, 155.
Faulkner, J., Roxburgh, I. W., and Strittmatter, P. A. 1968, *Ap. J.*, **151**, 203.
Fitzgerald, P. 1965, *Pub. David Dunlap Obs.*, **2**, 417.
Giuricin, G., Mardirossian, F., and Mezzetti, M. 1980, *Astr. Ap. Suppl.*, **39**, 255.
Giuricin, G., Mardirossian, F., Mezzetti, M., and Predolin, F. 1980, *Astr. Ap.*, **85**, 259.

Gordon, K. C. 1955, *A.J.*, **60**, 422.
Grønbech, B. 1976, *Astr. Ap. Suppl.*, **24**, 399.
Guinan, E. F., and Koch, R. H. 1977, *Pub. A.S.P.*, **89**, 74.
Gustafsson, B., and Nissen, P. E. 1972, *Astr. Ap.*, **19**, 261.
Gyldenkerne, K., Jørgensen, H. E., and Carstensen, E. 1975, *Astr. Ap.*, **42**, 306.
Habets, G. M. H. J., and Heintze, J. R. W. 1981, *Astr. Ap. Suppl.*, **46**, 193.
Hauck, B., and Mermilliod, M. 1980, *Astr. Ap. Suppl.*, **40**, 1.
Heard, J. F. 1965, *J. Roy. Astr. Soc. Canada*, **59**, 258.
Hilditch, R. W. 1975, *Mem. R.A.S.*, **79**, 101.
Hill, G., Hilditch, R. W., Younger, F., and Fisher, W. A. 1975, *Mem. R.A.S.*, **79**, 131.
Hiltner, W. A., Smith, B., and Struve, O. 1949, *Ap. J.*, **109**, 95.
Huruhata, M., Dambara, T., and Kitamura, M. 1953, *Ann. Tokyo Astr. Obs., Series 2*, Vol. 3, p. 227.
Jørgensen, H. E. 1979, *Astr. Ap.*, **72**, 356.
Jørgensen, H. E., and Gyldenkerne, K. 1975, *Astr. Ap.*, **44**, 343.
Law, Wai-Yuen, 1981, *Astr. Ap.*, **102**, 178.
Linnaluoto, S., and Piirola, V. 1979, *Astr. Ap. Suppl.*, **36**, 33.
Mancuso, S., Milano, L., and Russo, G. 1977, *Ap. Space Sci.*, **47**, 277.
Mardirossian, F., Mezzetti, M., Cester, B., Giuricin, G., and Russo, G. 1980, *Astr. Ap. Suppl.*, **39**, 235.
Mardirossian, F., Mezzetti, M., Predolin, F., and Giuricin, G. 1980, *Astr. Ap. Suppl.*, **40**, 57.
Margoni, R., Stagni, R., Mammano, A., and Illés-Almár, E. 1981, *Ap. Space Sci.*, **79**, 159.
McLean, B. J. 1982, *M.N.R.A.S.*, **201**, 421.
McNamara, D. H., Hansen, H. K., and Wilcken, S. K. 1971, *Pub. A.S.P.*, **83**, 192.
McNamara, D. H., and Powell, J. M. 1985, *Pub. A.S.P.*, **97**, 1101.

Mengel, J. G., Sweigart, A. V., Demarque, P., and Gross, P. G. 1979, *Ap. J. Suppl.*, **40**, 733.
Mezzetti, M., Cester, B., Giuricin, G., and Mardirossian, F. 1980, *Astr. Ap. Suppl.*, **39**, 265.
Miner, E. D., and McNamara, D. H. 1963, *Pub. A.S.P.*, **75**, 343.
Mochnacki, S. W. 1981, *Ap. J.*, **245**, 650.
Morgan, J. G., and Eggleton, P. P. 1979, *M.N.R.A.S.*, **187**, 661.
Nissen, P. E. 1970, *Astr. Ap.*, **6**, 138.
Northcott, R. J., and Bakos, G. A. 1956, *A.J.*, **61**, 188.
Olson, E. C. 1968, *Ap. J.*, **153**, 187.
Payne-Gaposchkin, C. 1946, *Ap. J.*, **103**, 291.
Perry, C. L. 1969, *A.J.*, **74**, 705.
Popper, D. M. 1943, *Ap. J.*, **97**, 394.
———. 1948, *Ap. J.*, **108**, 490.
———. 1950, *Pub. A.S.P.*, **62**, 115.
———. 1965, *Ap. J.*, **141**, 126.
———. 1966, *A.J.*, **71**, 175.
———. 1967, *Ann. Rev. Astr. Ap.*, **5**, 85.
———. 1968, *Ap. J.*, **154**, 191.
———. 1970, *Ap. J.*, **162**, 925.
———. 1971a, *Ap. J.*, **166**, 361.
———. 1971b, *Ap. J.*, **169**, 549.
———. 1981, *Ap. J.*, **244**, 541.
Rafert, J. B., and Wilson, R. E. 1984, *Ap. Space Sci.*, **100**, 117.
Roman, N. G. 1956, *Ap. J.*, **123**, 246.

Rucinski, S. M. 1976, *Pub. A.S.P.*, **88**, 777.
Rucinski, S. M., and Kaluzny, J. 1981, *Acta Astr.*, **31**, 409.
Rucinski, S. M., Whelan, J. A. J., and Worden, S. P. 1977, *Pub. A.S.P.*, **89**, 684.
Russo, G., Milano, L., D'Orsi, A., and Marcozzi, S. 1981, *Ap. Space Sci.*, **79**, 359.
Sanford, R. F. 1934, *Ap. J.*, **79**, 89.
———. 1937, *Ap. J.*, **86**, 191.
Snowden, M. S., and Koch, R. H. 1969, *Ap. J.*, **156**, 667.
Struve, O. 1944, *Pub. A.S.P.*, **56**, 34.
———. 1946, *Ap. J.*, **104**, 253.
———. 1947, *Ap. J.*, **106**, 92.
———. 1949, *Ap. J.*, **109**, 436.
Struve, O., and Gratton, L. 1948, *Ap. J.*, **108**, 497.
Struve, O., and Horak, H. G. 1950, *Ap. J.*, **112**, 178.
Struve, O., Horak, H. G., Canavaggia, R., Kourganoff, V., and Colacevich, A. 1950, *Ap. J.*, **111**, 658.
Struve, O., and Zebergs, V. 1959, *Ap. J.*, **130**, 137.
Tapia, S., and Whelan, J. 1975, *Ap. J.*, **200**, 98.
Van Hamme, W. 1982, *Astr. Ap.*, **116**, 27.
Whelan, J. A. J., Worden, S. P., and Mochnacki, S. W. 1973, *Ap. J.*, **183**, 133.
Wilson, R. E. 1978, *Ap. J.*, **224**, 885.
Wood, D. B. 1976, *A.J.*, **81**, 855.
Worden, S. P., and Whelan, J. A. J. 1973, *M.N.R.A.S.*, **163**, 391.
Yamasaki, A., and Kitamura, M. 1972, *Pub. Astr. Soc. Japan*, **24**, 213.

W. Van Hamme: School of Sciences, U.S.C. Coastal Carolina College, P.O. Box 1954, Conway, SC   29526

R. E. Wilson: Department of Astronomy, University of Florida, Gainesville, FL   32611